DNA-enhanced peroxidase activity of a DNA aptamer–hemin complex

Paola Travascio, Yingfu Li and Dipankar Sen

Background: *In vitro* selection (SELEX) previously identified short single-stranded DNAs that specifically bound *N*-methylmesoporphyrin IX (NMM), a stable transition-state analogue for porphyrin-metallation reactions. Interestingly, iron(III)-protoporphyrin (hemin) was a good competitive inhibitor for the DNA-catalyzed metallation reaction, and appeared to bind strongly to the NMM-binding DNA aptamers. We investigated the peroxidase activity of the aptamer–hemin complexes to see if the DNA component of the complex, like the apoenzymes in protein peroxidases, could enhance the low intrinsic peroxidatic activity of hemin.

Results: Two porphyrin-binding DNA aptamers bound hemin with submicromolar affinity. The aptamer–hemin complexes had significantly higher peroxidase activity than hemin alone, under physiological conditions. The V_{obs} of the *PS2.M*–hemin complex was 250 times greater than that of hemin alone, and significantly superior to a previously reported hemin–catalytic-antibody complex. Preliminary spectroscopic evidence suggests the coordination of the hemin iron in the complex changes, such that the complex more closely resembles horseradish peroxidase and other heme proteins rather than hemin.

Conclusions: A new class of catalytic activity for nucleic acids is reported. The aptamer–hemin complexes described are novel DNA enzymes and their study will help elucidate the structural and functional requirements of peroxidase enzymes in general and the ways that a nucleic acid 'apoenzyme' might work to enhance the intrinsic peroxidatic ability of hemin. These aptamer–hemin complexes could be regarded as prototypes for redox-catalyzing ribozymes in a primordial 'RNA world'.

Address: Institute of Molecular Biology & Biochemistry and the Department of Chemistry. Simon Fraser University, Burnaby, British Columbia, Canada, V5A 1S6.

Correspondence: Dipankar Sen
E-mail: sen@sfu.ca

Key words: catalytic DNA, DNAzyme, hemin, peroxidase, ribozyme

Received: **27 May 1998**
Revisions requested: **30 June 1998**
Revisions received: **30 July 1998**
Accepted: **3 August 1998**

Published: **25 August 1998**

Chemistry & Biology September 1998, **5**:505–517
http://biomednet.com/elecref/1074552100500505

 ISSN 1074-5521

Introduction

Metalloporphyrins are the active cofactors for a wide variety of enzymes and specialized cellular proteins. Heme [Fe(II)-protoporphyrin IX] is a cofactor used by proteins such as hemoglobin and myoglobin for reversible dioxygen binding. Heme also participates in the electron-transfer activity of cytochromes. Hemin [Fe(III)-protoporphyrin IX] (Figure 1a) is the active cofactor for a variety of enzymes, such as catalases, which degrade hydrogen peroxide, as well as a wide variety of oxidative enzymes such as peroxidases and monooxygenases (including the cytochrome P450 family) [1]. The iron (III) moiety within hemin has a single residual positive charge, which is neutralized by an anion, usually coordinated axially to the iron center. In its crystalline state hemin with an axial chloride ligand is generally called 'hemin' whereas the hydroxide form is designated 'hematin'. In the solution state however, these terms are often used interchangeably [2–4]. In this paper we use the nomenclature of the crystalline state, taking into account that the identity of axial ligands to the iron centre in solution might change, depending on the pH and other variables.

Peroxidases are enzymes that catalyze the oxidation of inorganic and organic substrates at the expense of an assortment of peroxides (ROOH — for example, hydrogen peroxide, alkyl hydroperoxides or acyl hydroperoxides [5]), according to the following scheme:

$$ROOH + AH_2 \rightleftharpoons ROH + A + H_2O$$

Many peroxidases are heme proteins, and utilize hemin as their cofactor. The essential steps of the peroxidatic cycle are shown in Figure 2 [6]. General peroxidase activity has, however, been detected in many different heme-proteins such as horseradish peroxidase [7], cytochrome c peroxidase, metmyoglobin, catalase and various cytochrome P450s (reviewed in [5]). In addition, it has long been known that hemin itself, as well as related compounds such as deuterohemin or coprohemin, are capable of catalyzing peroxidation reactions [8,9], although at much lower levels than those of hemin-utilizing enzymes, such as horseradish peroxidase [10]. Early studies showed that hemin could not only catalyze the decomposition of H_2O_2 [11], but also the oxidation of ascorbic acid [12]. The crucial elements of the peroxidation mechanism appeared

Figure 1

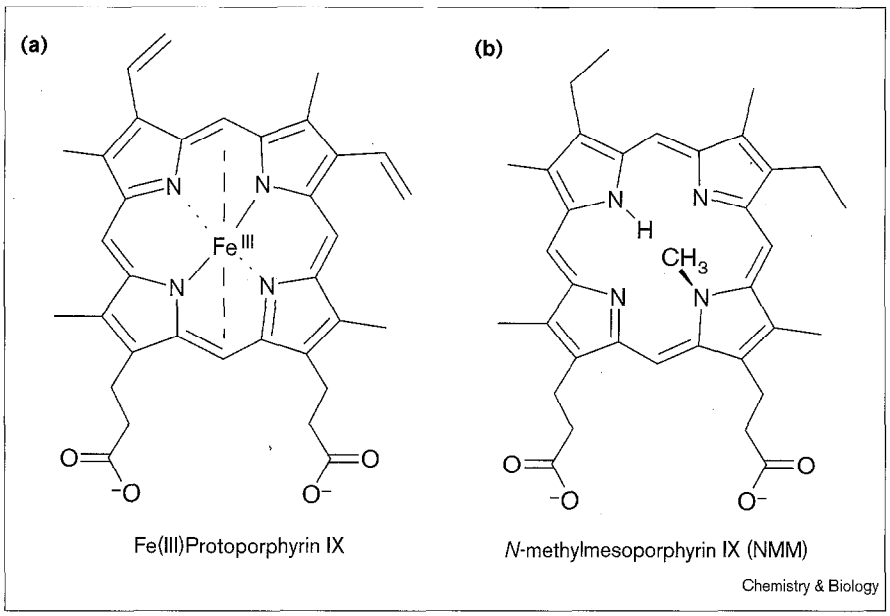

(a) Structure of iron (III)-protoporphyrin IX (with the iron center capable of axially binding two additional ligands). The fifth coordination site can be occupied by Cl^- or OH^-, giving respectively hemin or hematin. **(b)** Structure of *N*-methylmesoporphyrin IX (NMM).

to be the formation of primary and secondary complexes between hemin and H_2O_2, which were formed in two consecutive steps. These early kinetics studies were limited by complications due to the destruction of the hemin through oxidation, however [13–15]. A further caveat was that in aqueous solutions hemin aggregates significantly to form dimers and multimers, and that these latter species contribute poorly to the overall catalysis [16]. In recent years a variety of catalytic species, ranging from ferric salts to different metalloporphyrins, have been developed as model compounds for peroxidase-like activity. Most research has concentrated on horseradish peroxidase (HRP) itself (reviewed in [7]), however, and relatively little investigation of peroxidase mimics has been made. Very recently, an attempt was made to mimic the action of protein peroxidases by complexing hemin to amphiphilic water-soluble polymers [17]. Two classes of polymer 'carriers' were used, of which one, poly(sodium styrene-4-sulfonate-*co*-2-vinylnapthalene) (PSSS-N) had, in preliminary data, a degree of peroxidase activity (although it behaved poorly as a monooxygenase).

A key point of interest regarding protein peroxidases such as HRP has been: what does the apoenzyme (protein) component of such an enzyme contribute to make it such a superb catalyst (HRP is a diffusion-limited enzyme, with a k_{cat}/K_m value of $\sim 10^7\ M^{-1}s^{-1}$ [18])? Known contributions of the apoenzyme can be classified as follows. First, the protein supplies a key axial ligand to the ferric moiety of the hemin. In cytochrome P-450s, the axial ligand is a thiolate from cysteine (in the fifth coordination position, with the sixth open for peroxide binding) [19–24]. Peroxidases, however, use the imidazole moiety of a histidine residue as the axial ligand at the fifth coordination position [25,26]. This is similar to the situation in globins; in contrast to the globins, however, the Fe–N bond in peroxidases is both shorter and stronger, with the imidazole having a pronounced anionic or 'imidazolate' character and better electron donation properties. Second, the protein apoenzyme in peroxidases supplies a specific physical environment to the bound hemin. Although the hemin-binding site itself is undoubtedly hydrophobic, important ionizable residues have been identified on the distal side of the hemin, and these are thought to assist the heterolysis of the O–O peroxide bond [27]. A mechanistic hypothesis has been developed in which such ionizable groups are positioned in a precise stereochemical arrangement for participation as proton donors and acceptors, for neutralization of the developing charge density on the hemin, as well as for for stabilization of the higher valence states of the hemin iron [5]. Also, a distinct, distal histidine residue serves as both proton acceptor and donor to the peroxide oxygens, and an arginine residue stabilizes the negative charge that develops in the transition state for O–O heterolysis [25,26]. Such contributions are thought to be crucial for the very high catalytic efficiency of many peroxidase enzymes.

The above studies clearly support the idea that the protein environment of the hemin moiety in peroxidases exerts a specific and multifaceted enhancing role on the intrinsic peroxidatic property of the hemin. An interesting demonstration of this phenomenon with a non-natural hemin–protein complex was made by Cochran and Schultz [28], who discovered that a catalytic antibody for

Figure 2

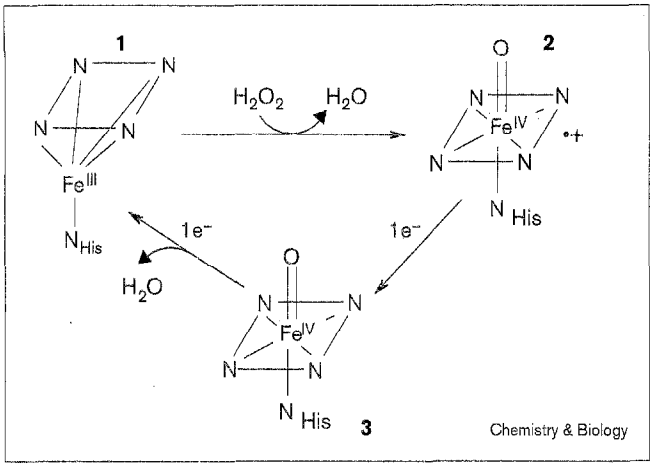

A peroxidation cycle, as for horseradish peroxidase-catalyzed reactions.

porphyrin metallation [29], derived for binding *N*-methylmesoporphyrin (a stable transition-state analogue for the porphyrin-metallation reaction) [30], also bound hemin with high affinity. This hemin–antibody complex was then found to exhibit enhanced peroxidase activity relative to hemin itself. More recently, a combinatorial approach has been used to mimic the structures of some natural heme proteins (four-helix bundles) [31,32]. The peroxidatic properties of these novel heme-binding proteins has not been reported, however.

We wished to investigate whether a completely different biomacromolecule, such as RNA or DNA, that has very different chemical functionalities from those found in proteins, could nevertheless form stable complexes with hemin, in which the nucleic-acid component could enhance the peroxidatic properties of the hemin in ways analogous to those found in protein peroxidases. There were two distinct rationales for carrying out such a study: first, to explore generally the mechanistic requirements of peroxidase enzymes, to see if functionalities other than those found in proteins could act to enhance the peroxidatic activity of hemin. The second point of interest was that such putative hemin–nucleic-acid complexes, if possessed of catalytic power greater than that of hemin itself, would constitute a novel class of ribozymes (or DNAzymes). This is of interest to the 'RNA world' hypothesis [33,34], which proposes a stage in evolution in which RNA molecules functioned as both catalysts and as carriers of genetic information. It is conceivable that in an RNA world ribozymes catalyzing metabolically important redox reactions might have recruited hemin or hemin-like molecules as cofactors.

In a previous study we had identified, using *in vitro* selection (SELEX), short-sequences of single-stranded

Table 1

Sequences of DNA oligomers used.

DNA aptamer	Sequence
PS5.M	5′-GTG GGT CAT TGT GGG TGG GTG TGG-3′
PS2.M	5′-GTG GGT AGG GCG GGT TGG-3′
BLD	5′-AAT ACG ACT CAC TAT AGG AAG AGA TGG-3′

DNA which, when folded, bound tightly to a variety of porphyrins, including hemin [35]. The selection had been carried out for binding to *N*-methylmesoporphyrin IX (NMM), a bent molecule that behaves as a stable transition-state analogue (TSA) for porphyrin metallation [30]. Like NMM, hemin has an 'off-planar' overall structure, with its ferric moiety sitting approximately 0.5 Å out of the plane of the porphyrin ring [36]. It was found that hemin was a good competitive inhibitor for the metallation reaction catalyzed by one of the NMM-binding DNA aptamers [37]. Moreover, bound hemin was useful for footprinting a number of the mentioned above NMM-binding aptamers [35].

The best characterized porphyrin-binding sequence was *PS5.M*, a 24-nucleotide DNA oligonucleotide. In later work, elements of rational design were used to design an 18-nucleotide sequence, *PS2.M*, which was an even more superior catalyst for porphyrin metallation (Y.L. and D.S., unpublished observations). Both *PS5.M* and *PS2.M*, whose sequences are given in Table 1, are guanine-rich. They appeared to form specific hemin-binding tertiary structures via the formation of intramolecular guanine quadruplexes [37,38]. The question we therefore wished to ask was: if indeed these single-stranded DNAs were able to form specific and tightly bound complexes with hemin, could such DNA–hemin complexes catalyze peroxidatic reactions to a greater extent than could hemin itself? And, if indeed they could, by what mechanism could they do so?

Results

Absorption spectra of hemin in the presence of Triton X-100

In order to study the peroxidatic activity of the DNA aptamer–hemin complexes, it was necessary first to measure the peroxidatic activity of free hemin (by itself, as well as in the presence of nonhemin-binding DNA oligomers). Hemin, however, is a highly hydrophobic molecule, with poor solubility in neutral and alkaline aqueous buffers. A number of studies have shown that the physical and chemical properties of aqueous hemin solutions can change in a manner consistent with aggregation [39–41]. In the case of protoporphyrin (the porphyrin moiety in hemin), the tendency to aggregation is acute, owing to the additional hydrophobic properties of the peripheral vinyl groups [42]. Stacked hemin dimers [40,41] and

Figure 3

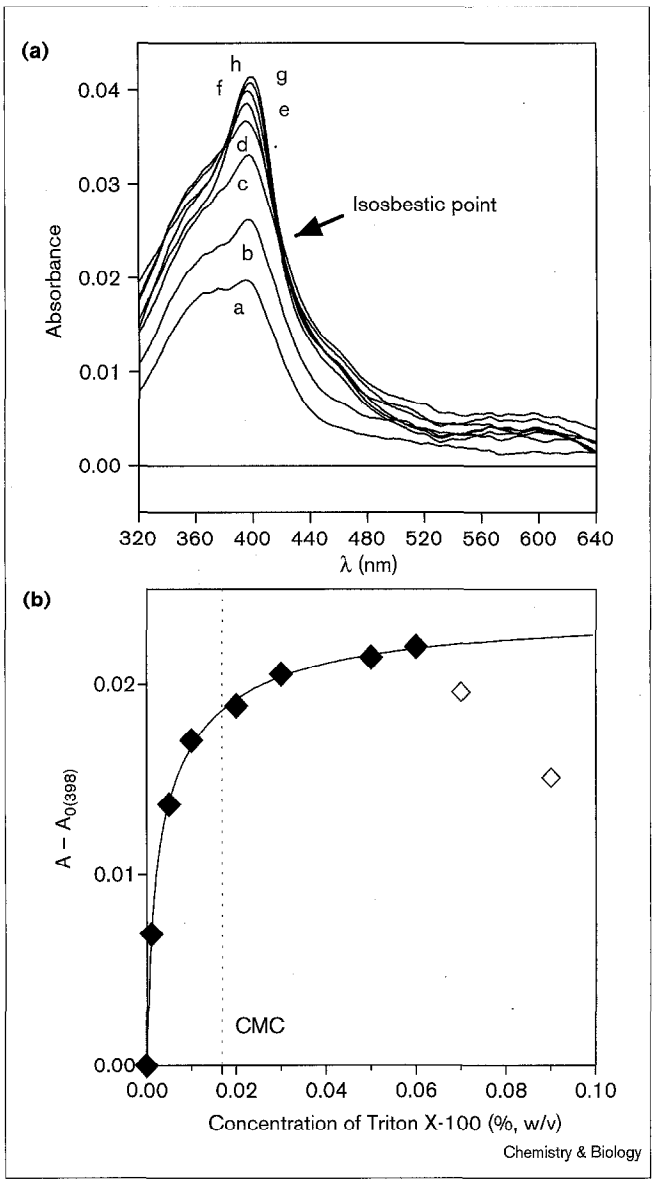

UV–visible spectra in the range of 320-700 nm of hemin (0.5 μM) with increasing detergent concentrations. Triton X-100 concentrations were: 0, 0.001, 0.005, 0.01, 0.02, 0.03, 0.05, and 0.06 % (w/v) from a–h, respectively. Baseline was subtracted from all curves. See the Materials and methods section for details. **(b)** The disaggregation of hemin (0.5 μM) as a function of Triton X-100 concentration. The CMC (critical micellar concentration) of Triton X-100 was 0.016% (w/v), and is indicated..

oligomers [43] have poor, if any, peroxidatic activity [16]. In addition, in the pH range of 7–13 hemin has the possibility of forming μ-oxo dimers [43], in which the iron centres of two hemin molecules are linked by an oxo bridge. The μ-oxo dimers do not display peroxidatic activity.

The mildest procedure for rendering hemins monomeric and soluble in aqueous buffers is to include low concentrations of non-ionic detergents, such as Triton X-100. Triton X-100 has, in fact, been widely used in studies of hemins *in vitro* [44]. We initially wished, therefore, to determine the minimal concentration of Triton X-100 that would satisfactorily disaggregate and solubilize low concentrations of hemin. Figure 3a shows the changes in the absorption spectra of 0.5 μM hemin in 40K buffer (see the Materials and methods section), in the presence of increasing concentrations of Triton X-100. Each experiment was repeated a number of times, and the spectra recorded only when equilibrium had been reached (in terms of stable, unchanging spectra) for specific hemin–Triton X-100 mixtures. Broadly, the spectra seemed to fall into two distinct regimes: with Triton X-100 concentrations from 0–0.01%, the spectra changed without any isosbestic points, consistent with the presence of multiple oligomeric species of hemin in the solution. At Triton X-100 concentrations higher than 0.01%, however, a clear isosbestic point appeared at 420 nm, suggesting that now two species existed in equilibrium — probably the monomeric and dimeric forms of hemin. Support for this hypothesis came from the observation that around 0.05% Triton X-100, the spectra did not increase any further, consistent with this absorbance reflecting a terminal, monomeric species. Figure 3b plots the measured absorbance at 398 nm as a function of Triton X-100 concentration. It can be seen that the absorption value began to plateau at Triton X-100 concentrations close to the critical micellar concentration (CMC) [45] for Triton X-100 (although decreases in absorbance were seen at very high Triton X-100 values). At around 0.05% Triton X-100, the absorbance of hemin had a molar extinction coefficient of $\varepsilon_{398} = 8.0 \times 10^4\ M^{-1}cm^{-1}$ (this value compared well with that reported for fully disaggregated hemin by Simplicio and Schewenzer [44] ($\varepsilon_{400} = \sim 6.5 \times 10^4\ M^{-1}cm^{-1}$). A slight red shift (2–3 nm) was noted for the detergent-disaggregated hemin.

The effect of *PS5.M* on the solubility and UV-visible spectra of hemin

The interaction of hemin with the DNA oligomer *PS5.M* (see Table 1) was now examined using absorption spectroscopy. Experiments were carried out in 40K buffer. Figure 4a shows the results of titrating 0.5 μM hemin (in the presence of 0.05% Triton X-100) with 0–1.5 μM *PS5.M* DNA. The presence of increasing concentrations of *PS5.M* was characterized by a sharp hyperchromism of the hemin Soret band, which also red shifted slightly from 398 nm to 404 nm at saturation (significantly, titration with a nonhemin-binding DNA oligomer, *BLD* [see Table 1] did not show these effects). The leveling off, or saturation, of the *PS5.M*-induced hyperchromism of the hemin Soret band was used to calculate the extinction coefficient for the DNA–hemin complex, which had a value of $\varepsilon_{404} = 1.9 \times 10^5\ M^{-1}cm^{-1}$. Scatchard analysis of the *PS5.M*– hemin interaction (data not shown) gave a ν value (moles of hemin bound per mole of DNA) of 0.77 ± 0.20, indicating a probable 1:1 binding stoichiometry.

Unlike the Triton X-100 data shown in Figure 3a, the spectroscopic transition from Triton X-100–hemin to *PS5.M*–hemin showed a monotonic hyperchromicity of the Soret band, with a well defined isosbestic point at 420 nm. This suggested that detergent–hemin and DNA–hemin complexes were the only two species involved in this equilibrium. When the same experiment was carried out in the absence of Triton X-100, no isosbestic point was seen, and the saturating absorbance of the Soret band was lower (ε_{404} = ~1.5×10^5 $M^{-1}cm^{-1}$; data not shown). These results suggested that low concentrations of detergent actually favoured the complexation of hemin with *PS5.M*, presumably because of a greater availability of monomeric hemin for complexation by the DNA. The data in Figure 4a were analyzed to determine the affinity between *PS5.M* and hemin, using the formalism described by Wang *et al.* [46] (see also the Materials and methods section). The value for the K_d obtained was 7 ± 2 nM. Hemin concentrations lower than 0.5 μM could not be used to obtain reliable absorption data, however. Moreover, iron porphyrins are known to be radiationless, so that fluorescence measurements with lower concentrations of hemin could not be made [47]. Therefore, the K_d value must be stated as being > 0.5 μM (although the real value was probably a great deal lower). The oligomer *PS2.M* appeared to bind hemin comparably well (data not shown).

Hyperchromicity of the Soret band has been considered to be an indicator of the hydrophobic nature of the hemin-binding site [48]. Presumably, this is also the case in the present system, with regard to the hemin-binding site within the folded *PS5.M*. Further discussion of the probable nature of the hemin-binding site in *PS5.M* is given below.

How does complex formation with the oligomers *PS5.M* and *PS2.M* affect the peroxidatic activity of hemin?

The peroxidatic activity of the *PS5.M*–hemin and *PS2.M*–hemin complexes (referred to hereafter as the 'catalyzed reaction') were tested, relative to the activity of hemin in the presence of equivalent concentrations of a nonheme-binding DNA oligomer, *BLD* (the 'background reaction'). Experiments were initially carried out in 40K buffer, which has a pH of 6.2 (40K was the optimal buffer for catalysis by *PS5.M* of the quite distinct porphyrin-metallation reaction [38]). Initial rates were measured by following absorbance at 414 nm ($\Delta\varepsilon = 3.6 \times 10^4$ $M^{-1}cm^{-1}$), the absorption maximum for the ABTS radical cation ($ABTS^{\cdot+}$). The data are shown in Figure 5. It can be seen that even under these unoptimized conditions the *PS2.M*–hemin and *PS5.M*–hemin complexes gave higher initial rates of ABTS oxidation than hemin in the presence of *BLD*. Both the background (in the presence of the *BLD* oligomer) and the DNA-catalyzed reactions were found to be zero order in ABTS concentrations (data not shown). As shown in Figure 5, however, both showed equivalent saturation behaviors with respect to hydrogen peroxide

Figure 4

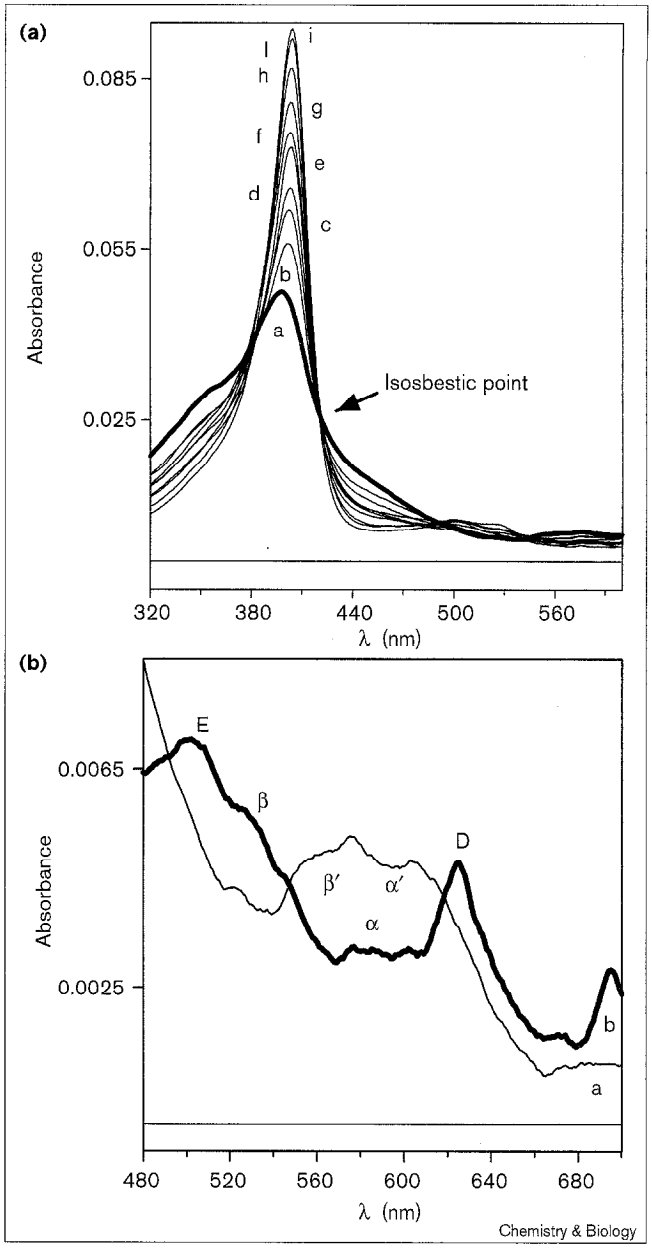

(a) Absorption titration of hemin (0.5 μM hemin, in the presence of 0.05% Triton X-100) with increasing concentrations of *PS5.M*, in the range of 320–700 nm. *PS5.M* concentrations were: 0, 0.1, 0.2, 0.3, 0.4, 0.5, 0.6, 0.8, 1.0, and 1.5 μM from a–l, respectively. **(b)** Visible spectra of free hemin in the presence of a nonbinding DNA, *BLD* (trace a) and the *PS5.M*–hemin complex in the absorption region of 480–700 nm (trace b). Samples a and b contained 0.5 μM hemin, 0.05% Triton X-100 and 1.0 μM DNA (whether *BLD* or *PS5.M*).

concentration. The k_{cat} and K_M values for all of the above reactions were calculated using GraphPad Prism™ 2.0 software. The background reaction had a k_{cat} value of 50 ± 2 min^{-1} and a K_M of 3.0 ± 0.3 mM (data points obtained from parallel sets of each experiment were found to agree within 5–8%). The K_M value was in good

Figure 5

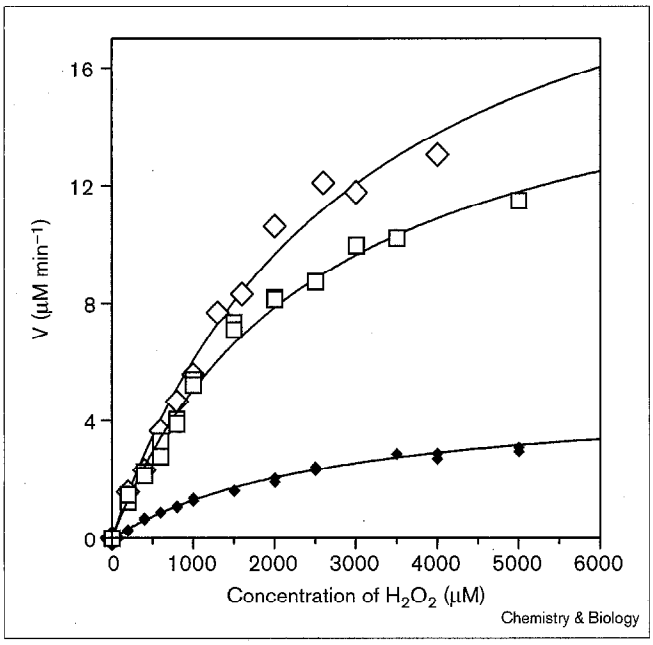

Michaelis–Menten plots for initial rates of peroxidation in the presence of different DNA oligomers. *PS2.M*–hemin catalyzed (◇); *PS5.M*–hemin catalyzed (□); the hemin background reaction, in the presence of the oligomer *BLD* (◆).

Figure 6

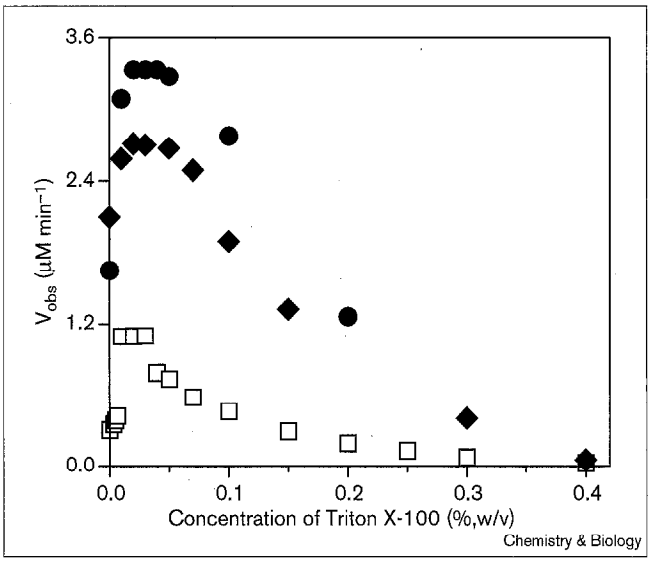

Dependence of the observed rates for peroxidation as functions of Triton X-100 concentration. *PS2.M*–hemin catalyzed (●); *PS5.M*–hemin catalyzed (◆); the hemin background reaction, in the presence of the oligomer *BLD* (□).

agreement with that reported for deuterohemin–peroxide complexes (3.4 mM) [9]. The *PS5.M*- and *PS2.M*-catalyzed reactions also fit well to the Michaelis–Menten formalism, and gave K_M values similar to the background (2.6 ± 0.5 mM and 2.9 ± 0.5 mM, respectively), but enhanced k_{cat} values. Under these unoptimized conditions, however the DNA-catalyzed rates were only approximately sixfold faster than the background. Even so, this rate acceleration was important given that these DNA-hemin complexes had not been selected for their peroxidatic activity, but rather for their ability to catalyze porphyrin metallation [35].

The above data are consistent with a kinetic scheme for H_2O_2-dependent peroxidation also described for other hemin-catalyzed peroxidations [9,12]. It involves a rapid pre-equilibrium between hemin and H_2O_2 that precedes the rate-determining formation of the activated peroxidatic complex (O=Hemin*):

$$\text{Hemin} + H_2O_2 \overset{K_M}{\rightleftharpoons} (\text{hemin}.H_2O_2) \overset{k_1}{\rightarrow}$$

$$\text{O=Hemin}^* \xrightarrow[+2AH_2]{k_2} \text{hemin} + \text{oxidized product}$$

An interesting observation was made about catalyzed and background reactions, namely that at H_2O_2 concentrations higher than ~3.6 mM the background (catalyzed by hemin alone) oxidized ABTS absorbances levelled off early, possibly due to the destruction and/or inactivation of the active hemin by excess H_2O_2. In the presence of the DNAzyme, however, initial rates curves were stable even at H_2O_2 concentrations exceeding 6 mM. It appeared likely that the hemin-binding site within the DNAzyme provided a degree of protection against the oxidative destruction of hemin [13].

We wished to determine whether the relatively low DNAzyme-catalyzed rates compared to the background rate, when measured in 40K buffer, could be enhanced under different conditions. We systematically examined, therefore, both the necessity for different buffer constituents, and the optimal concentrations of such components. Parameters such as pH and detergent concentration were also examined.

The effect of Triton X-100 on the background and DNA-catalyzed reactions

The presence of Triton X-100 was crucial to all our peroxidation assays, presumably to minimize the aggregation of hemin in our aqueous buffers. The need for Triton X-100 was especially critical for the measurement of the background rates. Figure 6 shows that the inclusion of detergent above its CMC (0.016%) dramatically stimulated both the background (in the presence of the DNA oligomer *BLD*) and the DNAzyme (*PS2.M* or *PS5.M*)-catalyzed peroxidations. The optimal Triton

X-100 concentrations in all cases appeared to be in the range 0.03–0.05% (w/v). Below 0.03% the background rates were found to be significantly variable — understandable in terms of hemin aggregation. By contrast, the DNAzyme-catalyzed reactions were stable and reproducible at all Triton X-100 concentrations. Hemin dimers exhibit very low peroxidase activity relative to monomers [16]. Therefore, Triton X-100-mediated shifts of the dimer–monomer equilibrium towards the monomer were probably responsible for the initial stimulatory effect of the detergent observed for both background and DNA-catalyzed reactions.

Interestingly, above 0.05% Triton X-100, the rates of both the catalyzed and background reactions declined with increasing detergent concentration. The decrease in the background initial velocities might be due to structural changes in the Triton X-100 micelles, which could lead to altered modes of interaction with bound hemin. As for the DNA-catalyzed reaction, although, as reported above, *PS5.M*'s affinity for hemin was much stronger than that of the detergent; very high Triton X-100 concentrations could begin to compete for and remove bound hemin from the DNA-bound complex. In support of this idea we found that the absorption profile of the DNA–hemin complex, as a function of Triton X-100, did show a progressive decrease above 0.05% Triton X-100, more or less mirroring the V_{obs} profile shown in Figure 6.

pH Dependence

Figure 7 shows the pH dependences of the background and *PS2.M*–catalyzed peroxidation reactions. The most notable pH sensitivity for both reactions was seen between pH values of 6.5 and 10. There was an approximately bell-shaped pH dependence for the background velocity, which peaked around pH 9. The pH trend followed by the *PS2.M*–hemin complex was similar, except that the bell-shaped dependence was much sharper, and peaked at pH 8.5. At this pH (8.5), optimal for the *PS2.M*–hemin complex, the complex-catalyzed reaction was measured to be ~20-fold faster than the background reaction. At pH 8.0 there was an even more optimal ratio of $V_{cat}/V_{background}$ (~50-fold). The trend followed by the *PS5.M*–hemin complex was similar, except that its rates were somewhat lower than those for the *PS2.M*–hemin complex. Given the above, the remainder of our experiments were carried out at pH 8.0.

Buffer effects

An analysis was made, at a fixed pH of 8.0, of the roles of different buffers on the *PS2.M*-catalyzed versus background reactions. These results are shown in Table 2. Both the catalyzed and background rates were found to be influenced by the nature of the buffer species. In general, nitrogenous buffers (with the exception of imidazole) appeared to support peroxidation, whereas certain oxyanion buffers appeared to have an inhibitory effect. Similar effects have been observed in the reactions of hemin with hydroperoxides [49,50] and with catalase and peroxidase enzymes [51,52]. The inhibitory effect of imidazole could be due to the very strong affinity of this compound for both axial positions of hemin. In

Figure 7

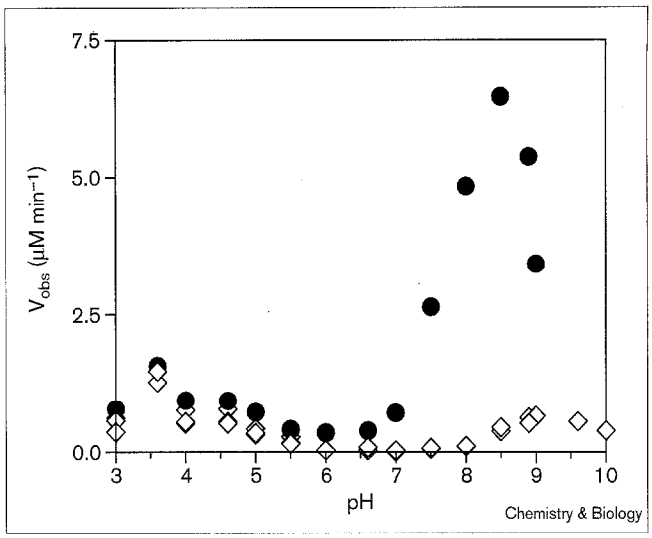

Dependence of the observed rates for *PS2.M*–hemin catalyzed (●) and hemin-catalyzed background (◊) peroxidations on pH. See the Materials and methods section for details.

Table 2

Dependence of rate parameters for *PS2.M*–hemin and Triton X-100 hemin peroxidations on buffers.

	Relative activity (%) = $V/V_{PS2.M\text{-}HepesNH_4OH} \times 100$	
Buffer	V_{cat}	V_{uncat}
Hepes-NH_4OH*	100	0.9
Hepes-NaOH*	50	1.4
Tricine-NH_4OH*	76	2.8
Tricine-NaOH*	48	1.7
Tris-HCl*	83	4.8
Tris-MES*	85	4.7
Tris-MES†	72	2.4
Na_2HPO4-NaH_2PO_4*	20	0.3
Imidazole-HCl*	~0	~0
Imidazole-H_2SO_4*	~0	~0

*Experimental conditions, pH = 8, 0.05% (w/v) Triton X-100, 1% (v/v) DMSO, 20 mM KCl. †Experimental conditions, pH = 8, 0.05% (w/v) Triton X-100, 1% (v/v) DMSO, 20 mM KOAc.

Figure 8

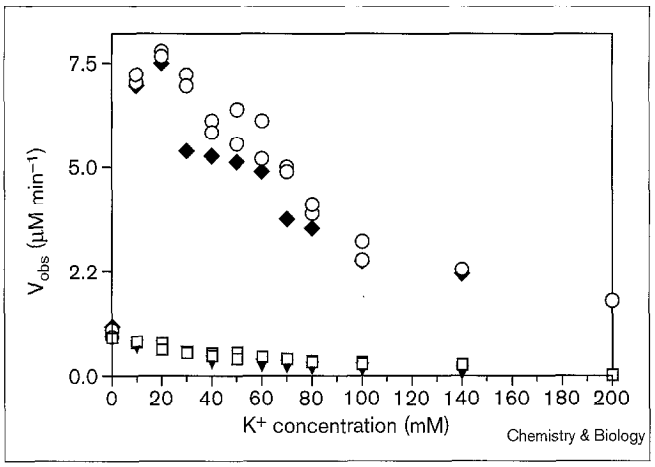

Peroxidation initial rates as functions of K^+ concentration. *PS2.M*–hemin catalyzed reactions in the presence of KCl (○) and KOAc (◆). Hemin (background) reactions with KCl (□) and KOAc (▼).

fact, the equilibrium constant for the formation of hemin–imidazole is 10–100-fold larger than those of many other nitrogenous bases. Thus, it could be that, under our experimental conditions, mono-ligand complexes formed with most nitrogenous bases whereas a bis-ligand complex was formed by imidazole. We found that in a HEPES–NH_4OH buffer (Table 2) the $V_{cat}/V_{background}$ ratio was maximized. This buffer was, therefore, used for subsequent optimization experiments.

Cation dependence

We investigated the effects of different cations, by themselves or in combination, on the DNAzyme-catalyzed and background reactions. In previous studies carried out on the porphyrin metallation activity of *PS5.M* [38], it had been found that K^+ was absolutely required for catalysis. Background and *PS2.M*-catalyzed peroxidations were therefore carried out in Tris-HCl, pH 8.0, containing variable concentrations (0–200 mM) of K^+. Figure 8 shows that at zero K^+ the DNAzyme (*PS2.M*)-mediated and background rates were essentially the same. The presence of as little as 10–20 mM K^+ enormously enhanced the DNAzyme-catalyzed reaction, whereas the background reaction changed very little. In fact, K^+ concentrations in the range of 10–25 mM appeared to be optimal for the *PS2.M*-catalyzed peroxidation reaction. These data were consistent with our earlier finding that K^+ was required for the correct secondary and tertiary folding of these guanine-rich DNAzymes into specific guanine-quadruplex structures, capable of binding porphyrins.

By contrast, in the presence of 20 mM Na^+ (in the absence of all K^+) as well as, separately, 0.1 mM Mg^{2+}, *PS2.M* was found, respectively, to be only 5% and 8% as active as in 20 mM K^+. The similarity in requirement for K^+ as opposed to Na^+ for the DNA-catalyzed metallation as well as DNA-catalyzed peroxidation reactions by *PS5.M* and *PS2.M* suggested that the same folded DNA structure was 'active' for the two quite different reactions.

Table 3

Dependence on Na^+ concentration (at fixed 20 mM K^+) of rate parameters for *PS2.M*–hemin and Triton X-100–hemin-mediated peroxidations.

Na^+ concentration (mM)	V_{cat}/V_{uncat}
0	105
4	64
12	80
20	97
40	95
60	130
100	250
200	> 250

Although K^+ was expected to play a specific structural role in stabilizing the active DNA conformations of the DNAzymes, we carried out titrations with Na^+ (with K^+ concentrations fixed at 20 mM), to see if there was a non-specific salt optimum for the DNA-catalyzed peroxidation. Table 3 summarizes that the presence of increasing concentrations of Na^+ in solution reduced both the catalyzed and background rates. The inhibitory effect appeared to be stronger on the background rate, so that the $V_{cat}/V_{background}$ ratio increased to > 250 at 200 mM Na^+. Because it was known that changes in the ionic strength could influence the extent of porphyrin dimerization and aggregation [53], we checked the absorption spectra of hemin through the entire range of Na^+ used (0–200 mM), to see if aggregation was in fact responsible for the decline seen in the background rate. We found, however, that the hemin spectra remained unchanged (and remained characteristic of the hemin monomer) throughout this Na^+ concentration range, indicating that the decrease in the rate of the background reaction at higher Na^+ levels was not a consequence of porphyrin aggregation (data not shown).

Discussion

What then was the mechanism of the DNA-enhanced catalysis? We have provided evidence that it was not simply a matter of the DNAzyme offering a binding site for hemin and therefore shifting the dimerization and oligomerization equilibria of hemin towards the monomeric (and catalytically active) form. Cochran and Schultz [28] reported a catalytic antibody for porphyrin metallation, which, when complexed with hemin, exhibited enhanced peroxidase activity. Their spectroscopic evidence (hyperchromicity of the Soret band) indicated

similar, and probably hydrophobic, binding sites for hemin in the antibody as in the DNAzymes reported here. The V_{obs} value they reported for their abzyme–hemin complex was, however, only ~twofold higher that for hemin itself [28]. The difference in the respective V_{obs} values of the abzyme–hemin and DNAzyme–hemin complexes could reflect differences in the outer sphere environment encountered by the bound hemin in the two cases.

A question could be posed as to whether the DNAzymes contributed anything more than a secure and hydrophobic binding site for the hemin. In an enzyme such as horseradish peroxidase (HRP), there are three major contributions of the protein apoenzyme to the catalytic power of the holoenzyme: firstly, a hydrophobic hemin-binding site. As indicated above, the DNAzymes appear to be able to supply such a site. Secondly, the protein component of HRP donates an axial ligand to the hemin iron, at the fifth position, via a histidine residue. This axial ligand is crucial in donating electron density to the iron [21]. In the case of the DNAyzmes, is it conceivable that a guanine residue could be acting as a ligand? Further mutagenesis experiments and experiments involving chemical interference procedures will have to be used to answer this question. Thirdly, in HRP, a third major contribution of the protein is to the distal side of the hemin (the side of the porphyrin ring on which the oxo complex forms). This face of the hemin-binding pocket in HRP is quite polar, and there are several potential hydrogen-bond acceptors and donors. In the case of the DNAzymes, such a function is also conceivable. Very likely the hemin intercalates, to a degree, between two guanine quartets. Although the surface of a guanine quartet is, on the whole, hydrophobic, both the interior of the quartet and the sugar-phosphate backbones of the DNA would present polar environments (reviewed in [54]) that could carry out the above functions.

In support of the above points, we were able to draw certain preliminary conclusions by comparing the absorption spectra of hemin and the *PS5.M*–hemin complex with spectra taken in earlier studies on two other porphyrins: mesoporphyrin IX (MPIX), *N*-methylmesoporphyrin IX (NMM), and their respective DNAzyme complexes [55,56]. MPIX was both poorly soluble and aggregation-prone, as, indeed, was the case for hemin. The spectra of MPIX fully dispersed in Triton X-100, however, as well as spectra of MPIX fully bound to *PS5.M*, were found to have very similar absorption intensities in the Soret region (~400 nm). NMM was both more soluble and less aggregated than either hemin or MPIX. Furthermore, it bound to *PS5.M* with nanomolar affinity (like hemin, but unlike MPIX, which bound with micromolar affinity). It was found nevertheless that the spectra of NMM in the absence of Triton X-100, in the presence of Triton X-100, as well as when bound to the DNAzyme, were all comparable to one another in terms of the intensity and shape of the Soret band (although the complex had a slight red shift relative to free NMM).

In contrast to the above, the intensity of the Soret band for the *PS5.M*–hemin complex was enhanced by as much as twofold relative to hemin disaggregated fully by Triton X-100 (see Figure 4). It is well known that the interaction of the metal centre in metalloporphyrins with axial ligands has a profound impact on the chemical and physical properties of the metalloporphyrins. In a series of studies, Corwin *et al.* [57] showed that both the visible and near-visible electronic transitions of hemin were affected by stereoelectronic interactions between ligands bonded to the metal and the porphyrin π electrons. It was found that the Soret band maximum shifted to longer wavelengths and increased in intensity as a consequence of the metalloporphyrin metal center interacting with strong ligands. The red-shift and hyperchromicity observed in the Soret band in the *PS5.M*–hemin interaction (above) are intriguing; it is still premature, however, to suggest that this might indicate an axial ligand supplied by the DNA to the metal center of the bound hemin. Further experiments will have to be carried out to investigate this possibility.

With regard to the spin and overall coordination characteristics of the hemin iron centre, it was interesting to examine the differences between the spectra of hemin in Triton X-100, and when bound to the DNAzyme. The visible spectra (480–700 nm), shown in Figure 4b, were particularly informative, because the pattern and the location of the absorption maxima were utterly distinctive in the two cases. Table 4 summarizes this information. Basically, an α'–β' pattern of peaks of hemin in Triton X-100 (identifiable with the α and β bands typical of free metalloporphyrins [58]) transformed to a more complex pattern of E–α– β–D (nomenclature adopted from Saunders *et al.* [58]) in the presence of increasing concentrations of *PS5.M*. Bands D and E usually occur together and are characteristic of ferric hemoproteins; these peaks are generally accepted to reflect ligand-to-metal charge transfer transitions. Therefore, the new E–α–β–D peak pattern for *PS5.M*, distinct from α'–β', indicated a different kind of

Table 4

Absorption parameters of hemin complexes in the visible region.

Hemin Complex	α, nm (ε_M)	β, nm (ε_M)	D, nm (ε_M)	E, nm (ε_M)	Spin
Triton X-100	600 (1.1×10^4)	560 (1.1×10^4)	–	–	LS
PS5.M	580 (6.0×10^3)	530 (1.0×10^4)	625 (1.0×10^4)	500 (1.5×10^4)	HS

Table 5

Comparison of absorption parameters of different hemin complexes.

Enzyme	Soret		E band	D band		Spin/ Coord.
	λ (nm)	ε_M	λ (nm)	λ (nm)	ε_M	
HRP	402	1.05×10^5	497	645	0.28×10^4	HS/5C
Cyt c Perox	408	1.0×10^5	505	645	0.3×10^4	HS/5C
Heme-ox	404	$1.65 \infty 10^5$	500	631	1.1×10^4	HS/6C
Met Hb	405	1.79×10^5	500	631	0.44×10^4	HS/6C
Met Mb	408	1.88×10^5	502	630	0.4×10^4	HS/6C
PS5.M	404	1.9×10^5	500	625	1.0×10^4	HS/6C

See [60] for protein parameters.

axial coordination for hemin in the *PS5.M* complex. Interestingly, comparison of the full absorption spectra of the *PS5.M*–hemin complex with those of MetHb.(H_2O) and MetMb.(H_2O) (assumed to ligate via histidine) [59,60], as well as that of heme-heme oxygenase [61] indicated that both the peak positions and the extinction coefficients were remarkably similar (see Table 5). These heme proteins are known to be six-coordinate high-spin species (bands at ~500 and 620–630 nm are considered typical of high-spin ferric state [62]). We therefore postulate that the iron(III) moiety in the DNAzyme–hemin complex (measured at pH 6.2) is also in the high-spin state.

As to whether the ferric moiety has a fivefold or sixfold ligand coordination, the Soret band again provides some preliminary information. From studies carried out on metmyoglobin [63] and yeast cytochrome c peroxidase [64], a generalized spectroscopic characterization of penta- and hexa-coordinated high-spin ferric proteins has been formulated. Two major features appear to be: hexa-coordinated compounds exhibit intense Soret bands with extinction coefficients of $>1.2 \times 10^5\ M^{-1}cm^{-1}$; and the D bands are blue-shifted, along with increases in intensity. Table 5 summarizes the known data for a number of heme proteins. Using this preliminary analogy, the DNAzyme–hemin complex appears to be hexa-coordinated. At this point in our studies, however, we can only speculate about the nature of the two putative ligands. At least one of the two positions might be occupied by water. The observed pH dependence of the DNA-catalyzed peroxidation might provide support for such a water ligand, and this is an area that we are currently investigating with a range of spectroscopic and other experiments.

The data presented above demonstrated, first, that the DNA-catalyzed peroxidation reaction was contingent on the specific binding of hemin to specific DNA oligomers. In the presence of nonhemin-binding DNA oligomers, such as *BLD*, no catalysis above that of hemin itself was observed. Moreover, the DNA-mediated catalysis was absolutely dependent on the hemin-binding DNA oligomers (*PS2.M* and *PS5.M*) forming specific folded structures. In the absence of solution conditions favouring such folded structures (such as the absence of K^+ but the presence of compensating concentrations of Na^+) *PS2.M* and *PS5.M* did not show any catalysis above the background level.

The *PS2.M*–hemin complex defines a new kind of cofactor-utilizing catalytic nucleic acid, in which the nucleic acid moiety utilizes hemin to catalyze oxidative chemistries. Above, we have provided evidence that the nucleic acid 'apoenzyme' contributes significantly to enhance the intrinsic catalytic capability of the cofactor. These data provide new insight into our conception of the 'RNA world', by adding redox reactions to the repertoire of nucleic-acid-catalyzed reactions.

Significance

In this paper we report a new category of nucleic-acid enzyme. We report that DNA aptamers complexed tightly to hemin show peroxidase activity two orders of magnitude higher than that of hemin (whether aggregated or monomeric), and also significantly greater than that of a previously described catalytic antibody–hemin complex. We provide evidence that a nucleic acid 'apoenzyme' can thus contribute significantly to improve the intrinsic catalytic capability of the hemin cofactor. Preliminary spectroscopic evidence indicates that in our DNAzymes the DNA host might be contributing in more than one way to the enhancement of the catalytic rate. These data provide new insight into the concept of a primordial 'RNA world', by adding redox reactions to the repertoire of nucleic-acid-catalyzed reactions.

Materials and methods

Porphyrins

Porphyrins [iron(III)protoporphyrin IX and mesoporphyrin IX] were purchased from Porphyrin Products (Logan, UT), and used without further purification. Stock solutions (5 mM) were prepared by dissolving accurately weighed amounts of porphyrin in 1 ml of dimethylsulfoxide (DMSO) and shaking until fully dissolved (the dissolution was monitored by centrifugation and by absorbance checks as functions of time). Diluter stock solutions (100 μM), were made up in DMSO and frozen in the dark at −20°C. These diluter stocks were found to be stable for approximately one week (as assayed by absorbance) [65,66]. For the experiments described in this paper, final aqueous solutions (containing 0.1–0.5 μM porphyrin) were prepared freshly for each experiment, by diluting appropriate volumes from the 100 μM stocks into the appropriate aqueous buffers.

Hydrogen peroxide 3% (w/v), in stabilized form, was purchased from VWR Canlab. 2,2'-azinobis(3-ethylbenzothiozoline)-6-sulfonic acid (ABTS) was obtained as the diammonium salt from Sigma, and used without further purification. Triton X-100 was from Sigma. All chemicals used were of reagent grade.

DNA oligomers

DNA oligomers were synthesized at the University Core DNA Service at the University of Calgary. Synthesized DNA sequences were size-purified in preparative polyacrylamide gels, following which eluted DNA was re-purified on Spice C18 columns (Rainin). Following lyophilization, purified DNA oligomers were dissolved in TE buffer (10 mM Tris, pH 7.5; 0.1 mM EDTA) and stored at −20°C. The concentrations of the DNA oligomers were determined from absorbance measurements at 260 nm (with 1 O.D. taken to be 35–40 μg/ml DNA, depending on the oligomer). The sequences of the DNA oligomers used in this study are shown in Table 1.

Spectroscopy

Absorption spectra were recorded in a dual-beam Cary 3E UV–Visible Spectrophotometer, at 20° ± 1°C.

Formation of actively folded DNA molecules

DNA oligomers from frozen stock solutions (above) were thawed, heated at 95°C for 5 min (in TE buffer), and then slowly cooled back to ambient temperature. The DNA was now made up to final buffer salt concentrations, and allowed to sit for 30 min at room temperature to allow proper folding. Where a porphyrin was to be added it was done so from 100 μM stocks in DMSO (see above). The added porphyrin was allowed to complex with DNA over a 20 min incubation (deemed by absorbance changes to be a sufficient time for complex formation). Peroxidation and other assays were carried out subsequent to this complex formation.

Binding assays

Titration of hemin with Triton X-100: Hemin 0.5 μM was freshly diluted from a DMSO stock into a number of tubes containing 40K buffer (50 mM MES, pH 6.2; 100 mM Tris acetate, 40 mM potassium acetate, 1% [v/v] DMSO), but containing different concentrations of Triton X-100 (diluted from a 5% ,w/v, stock solution). The solutions were allowed to equilibrate for 10–15 min, and their spectra were recorded over the wavelength range of 320–700 nm. It was particularly important to make up each hemin–Triton solution separately; attempts to titrate a single solution of hemin by sequential additions of detergent led to spectra that were noisy. The above procedure, by contrast, gave consistently reproducible spectra.

Titration of hemin with DNA oligomers: Different concentrations of DNA oligomers were first incubated individually in the 40K+T buffer (40K buffer containing 0.05% Triton X-100 – a sufficient Triton X-100 concentration to retain hemin in its monomeric form). All solutions were then made up to 0.5 μM hemin (see above), and spectra were recorded in the range of 320–700 nm.

Calculation of binding constants

DNA oligomers: The saturation curve for the complexing of hemin to folded DNA oligomers was determined by plotting absorbance changes in the Soret band (at 404 nm) as a function of DNA concentration. The dissociation constant (K_d) was obtained by fitting the saturation plot with the following equation described by Wang *et al.* [46]:

$$[DNA]_o = K_d\,(A-A_o) / (A_\infty-A) + [P_o]\,(A-A_o) / (A_\infty-A_o)$$

Where $[DNA]_o$ is the initial concentration of DNA; $[P_o]$ is the initial concentration of monomeric hemin; and A_∞, and A_o represent hemin absorbances at, respectively, saturating DNA concentrations, and in the absence of DNA but in the presence of a saturating concentration (~0.05%) of Triton X-100.

Kinetic measurements: Kinetics were followed by monitoring the appearance of the ABTS radical cation ($ABTS^{\bullet+}$) at 412 nm, using a dual-beam Cary 3E UV-visible spectrophotometer thermostatted at 20° ± 1°C. *The* $\Delta\varepsilon$ *value used was* 36,000 M^{-1} cm^{-1} [67]. Sample cuvettes (1 ml) contained buffer, hemin (or the DNA–hemin complex), ABTS, and Triton X-100 or salts. Reactions were initiated by the addition of H_2O_2, and increases in absorbance at 414 nm were measured as a function of time. Some of the kinetic measurements were repeated using two different kind of blanks: in one, the reference cuvette contained buffer and catalyst (hemin or DNA–Hemin) but no ABTS; in the other, the reference cuvette contained buffer and ABTS but no catalyst. In both instances, the addition of H_2O_2 gave identical observed catalyzed rates. These results suggested that ABTS was oxidized only very slowly by H_2O_2 in the absence of a catalyst, and that such a catalyst-free oxidation did not contribute significantly to the overall oxidation rate measured in the presence of either catalyst (either hemin or a hemin–aptamer complex).

For kinetics studies carried out at pH 6.2, the rate of change of A_{414} was linear over 5 min for both the DNA–hemin 'catalyzed' and the 'background' (hemin–catalyzed) peroxidations. At pH 8.1, however, the radical cation could not be monitored reproducibly for times longer than 1 min, owing to further transformations of the radical cation [49–68]. Therefore, for background rates at pH 8.1, measurements were taken within the regime of linear absorbance change seen during the first minute of reaction whereas for DNA-catalyzed reactions the initial rates were calculated from the slope of the initial linear portion of the increase in absorbance. Most experiments were repeated at least two times, and were found to agree within ± 5–10%.

Protocols for peroxidation experiments

Effect of Triton X-100: Peroxidation reactions were carried out at 20° ± 1°C, in 40K buffer (with various concentrations of Triton X-100 added – see below), with 5 mM ABTS, 0.1 μM catalyst (hemin or DNA–hemin complex) and 600 μM H_2O_2 (from stock). Reactions were initiated by addition of H_2O_2. Triton X-100 concentrations in the 40K buffer were varied from 0%–0.4%.

pH dependence: The reactions were carried out at 20°C ± 1°C in buffers at different pH values (but containing invariably 40 mM KOAc, necessary for DNA folding). All buffers also contained 0.05% Triton X-100, 1% DMSO, 5 mM ABTS and 0.1 μM catalyst. The reactions were initiated with H_2O_2 added to 600 μM (final). Buffer materials of highest purity available were used. Glycine-HCl was used for pH range 3.0-3.6; sodium acetate buffer for pH 4.0-5.5; sodium phosphate buffer for pH 6.0-7.0; Tris-HCl for pH 7.5-9.0; and glycine-NaOH for pH 9.0-10.0 [55].

Cation dependence: Potassium–dependence reactions were carried out in Tris-HCl buffer (25 mM Tris, pH 8.0, 0.05% Triton X-100, and 1% DMSO), with 0.1 μM catalyst, and 5 mM ABTS. Reactions were initiated with the addition of H_2O_2 to 600 μM (final). Reactions carried out in Na^+ (0–200 mM), or in magnesium (0–1 mM), were carried out under similar conditions, except that the buffer used was 25 mM HEPES-NH_4OH, pH 8.0. For the above experiments, the common anion used was chloride. For the K^+ dependence experiments, however, parallel measurements were carried out with both chloride and acetate anions.

Buffer dependence: The reaction rates were measured in the presence of several different buffers, all at pH 8.0. The solutions contained, respectively, 25 mM Tris, Tricine, HEPES, imidazole and phosphate. In addition, the reaction cocktail contained 0.05% Triton X-100, 1% DMSO, 0.1 μM catalyst, 5 mM ABTS, 600 μM H_2O_2 and 20 mM KCl (necessary for the active folding of DNA), except where specified otherwise.

Acknowledgements

This work was supported by the Natural Sciences and Engineering Research Council (NSERC) of Canada, and by the British Columbia Health Research Foundation (BCHRF). We are grateful to Andrew Bennet, David Dolphin, Andrew Yim, Jenny Lum and the members of the Sen lab for discussions.

References

1. Sheldon, R.A. (1981). *Metal-catalyzed Oxidations of Organic Compounds.* pp. 216-268, Academic Press, New York.
2. Beppu, M., Nagoya, M. & Kikugawa, K. (1986). Role of heme compounds in the erythrocyte membrane damage induced by lipid hydroperoxides. *Chem. Pharm. Bull.* **34**, 5063-5070.
3. Tappel, A.L. (1953). The mechanism of oxidation of unsaturated fatty acids catalyzed by hematin compounds. *Arch. Biochem. Biophys.* **44**, 378-395.
4. Dix, T.A. & Marnett, L.J. (1985). Conversion of linoleic acid hydroperoxide to hydroxy, keto, epoxy hydroxy, and trihydroxy fatty acids by hematin. *J. Biol. Chem.* **260**, 5351-5357.
5. Marnett, L.J., Weller, P. & Battista, J.R. (1986). Comparison of the peroxidase activity of hemeproteins and cytochrome P-450. In *Cytochrome P-450.* (Ortiz de Montellano, P.R., ed.), pp. 29-76, Plenum Press, New York.
6. Marnett, L.J. & Kennedy, T.A. (1995). Comparison of the peroxidase activity of hemeproteins and cytochrome P450. In *Cytochrome P450.* (Ortiz de Montellano, P.R., ed.), pp. 49-80, Plenum Press, New York.
7. Dunford, H.B. & S., S.J. (1976). On the function and mechanism action of peroxidases. *Coord. Chem. Rev.* **19**, 187-251.
8. Kelly, H.C., Davies, M.D., Mantle, D. & Jones, P. (1977). Hydroperoxidase activities of ferrihemes: heme analogues of peroxidase enzyme intermediates. *Biochemistry* **16**, 3974-3978.
9. Portsmouth, D. & Beal, E.A. (1971). The peroxidase activity of deuterohemin. *Eur. J. Biochem.* **19**, 479-487.
10. Saunders, B.C., Holmes-Siadle, A.G. & Stark, B.P. (1964). *Peroxidase*, pp. 169-181, Butterworths, London.
11. Kremer, M.L. (1965). Decomposition of hydrogen peroxide by hemin. *Trans. Faraday. Soc.* **61**, 1453-1459.
12. Kremer, M.L. (1967). Hemin-catalyzed oxidation of ascorbic acid by H_2O_2. *Trans. Faraday Soc.* **63**, 1208-1214.
13. Brown, S.B., Jones, P. & Suggett, A. (1968). Reactions between haemin and hydrogen peroxide. *Trans. Faraday Soc.* **64**; 986-993.
14. Brown, S.B. & Jones, P. (1968). Reactions between haemin and hydrogen peroxide. *Trans. Farday Soc.* **64**, 994-998.
15. Brown, S.B. & Jones, P. (1968). Reactions between haemin and hydrogen peroxide. *Trans. Farday Soc.* **64**, 999-1005.
16. Brown, S.B., Dean, T.C. & Jones, P. (1970). Catalytic activity of iron(III)-centred catalyst. *Biochem. J.* **117**, 741-744.
17. Johnstone, R.A.W., Simpson, A.J. & Stocks, P.A. (1997). Porphyrins in aqueous amphiphilic polymers as peroxidase mimics. *Chem. Commun.*, 2277-2278.
18. Saunders, B.C. (1964). *Peroxidase*, pp. 60-70, Butterworths, London.
19. Dawson, J.H., Sono, M., Hall, K. & Hager, L.P. (1986). Ligand and halide binding properties of chloroperoxidase: peroxidase-type active site heme environment with cytochrome P450 type endogenous axial ligand and spectroscopic properties. *Biochemistry* **25**, 347-356.
20. Dawson, J.H. & Sono, M. (1987). Cytochrome P450 and chloroperoxidase: thiolate-ligated heme enzymes. spectroscopic determination of their active site structures and mechanistic implications of thiolate ligation. *Chem. Rev.* **87**, 1255-1276.
21. Dawson, J.H. (1988). Probing structure–function relations in heme-containig oxygenases and peroxidases. *Science* **40**, 433-439.
22. Champion, P.M., Stallard, B.R., Wagner, G.C. & Gunsalus, I.C. (1982). Resonance raman detection of an Fe-S bond in cytochrome P-450cam. *J. Am. Chem. Soc.* **104**, 5469-5472.
23. Hahn, J.E., Hodgson, K.O., Andersson, L.A. & Dawson, J.H. (1982). Endogenous cysteine ligation in ferric and ferrous cytochrome P-450. *J. Biol. Chem.* **257**, 10934-10941.
24. Kau, L.S., Svastits, E.W., Dawson, J.H. & Hodgson, K.O. (1986). Iron-sulpur bond lenghts in ferrous-CO heme complexes as function of sulpur donor type. *Inorg. Chem.* **25**, 4307-4309.
25. Poulos, T.L. & Kraut, J. (1980). The stereochemistry of peroxidase catalysis. *J. Biol. Chem.* **255**, 8199-8205.
26. Poulos, T.L. (1988). Heme enzyme crystal structures. In *Advances in Inorganic Biochemistry.* (Eichhorn, G.L. & Marzilli, L.G., eds.), pp. 1-36, Elsevier Publishing Co., Amsterdam.
27. Dunford, H.B. (1982). Peroxidases. In *Advances in Inorganic Biochemistry.* (Eichhorn, G.L. & Marzilli, L.G., eds.), pp. 41-68, Elsevier Publishing Co., Amsterdam.
28. Cochran, A.G. & Schultz, P.G. (1990). Peroxidase activity of an antibody–heme complex. *J. Am. Chem. Soc.* **112**, 9414-9415.
29. Cochran, A.G. & Schultz, P.G. (1990). Antibody-catalyzed porphyrin metallation. *Science* **249**, 781-783.
30. Schultz, P.G. & Lerner, R. A. (1995). From molecular diversity to catalysis: lessons from the immune system. *Science* **269**, 1835-1842.
31. Hecht, M.H., Shieh, H.M., Buckwalter, B.L. & Xiong, H. (1995). Periodicity of polar and nonpolar amino acids in the major determinant of secondary structure in self-assembling oligomeric peptides. *Proc. Natl Acad. Sci. USA* **92**, 6349-6353.
32. Hecht, M.H., *et al.*, & Rojas, N.R. (1997). *De novo* heme proteins from designed combinatorial libraries. *Protein Sci.* **6**, 2512-2524.
33. Gilbert, W. (1986). The RNA World. *Nature* **319**, 618.
34. Joyce, G.F. & Orgel, L.E. (1993). Prospects for understanding the origin of the RNA world. In *The RNA World.* (Gesteland, R.F., Atkins, J.F., eds), pp. 1-25, Cold Spring Harbor Laboratory Press, New York.
35. Li, Y., Geyer, C.R. & Sen, D. (1996). Recognition of anionic porphyrins by DNA aptamers. *Biochemistry* **35**, 6911-6922.
36. Koenig, D.F. (1955). The Structure of a-Chlorohemin. *Acta Crystallogr.* **18**, 663-673.
37. Li, Y., & Sen, D. (1996). A catalytic DNA for porphyrin metallation. *Nat. Struct. Biol.* **3**, 743-747.
38. Li, Y. & Sen, D. (1997). Towards an efficient DNAzyme. *Biochemistry* **36**, 5589-5599.
39. Brown, S.B., Dean, T.C. & Jones, P. (1970). Aggregation of ferrihaems. *Biochem. J.* **117**, 733-739.
40. Phillips, J.N. (1963). Physicochemical properties of porphyrins. In *Comprehensive Biochemistry.* (Florkin, M. & Stotz, E.H., eds.), pp. 34-72, Elsevier Publishing Co., Amsterdam.
41. Falk, J.E. (1963). Chemistry and biochemistry of porphyrins and metalloporphyrins. In *Comprehensive Biochemistry.* (Florkin, M. & Stotz, E.H., eds.), pp. 3-33, Elsevier Publishing Co., Amsterdam.
42. Brown, S.B., Prudhoe, K. & Jones, P. (1974). Equilibrium and kinetic studies of deuteroferrihaem dimerization. *J. Chem. Soc. Dalt. Trans.*, 911-913.
43. White, W.I. (1978). Aggregation of porphyrins and metalloporphyrins. In *The Porphyrins.* (Dolphin, D., ed.), pp. 303-335, Academic Press, New York.
44. Simplicio, J. & Schwenzer, K. (1973). Hemin intercalated in micellar CetMe3NBr and Triton X-100. A kinetic, spectral, and equilibrium study with cyanide. *Biochemistry* **12**, 1923-1929.
45. Fendler, J.E. & Fendler, J.H. (1970). Micellar catalysis in organic reactions: kinetic and mechanistic implications. *Adv. Phys. Org. Chem.* **8**, 271-406.
46. Wang, Y., Hamasaki, K. & Rando, R.R. (1997). Specificity of aminoglycoside binding to RNA constructs derived from the 16S rRNA decoding region and the HIV–RRE activator region. *Biochemistry* **36**, 768-779.
47. Gouterman, M. (1978). Optical spectra and electronic structure of porphyrins and related rings. In *The Porphyrins.* (Dolphin, D., ed.), pp. 1-165, Academic Press, New York.
48. Slome-Schwok, A. & Lehn, J.M. (1990). Interaction of porphyrin-containing macrotetracyclic receptor molecule with single-stranded and double-stranded polynucleotides. A photophysical study. *Biochemistry* **29**, 7895-7903.
49. Bruice, T.C. & Almarsson, O. (1995). A homolytic mechanism of O–O bond scission prevails in the in the reaction of alkyl hydroperoxides with an octacationic tetraphenylporphyrinato-iron(III) complex in aqueous solution. *J. Am. Chem. Soc.* **117**, 4533-4544.
50. Bruice, T.C., Beck, M.J. & Gophinat, E. (1993). Influence of nitrogen base ligation on the rate of sulphonatedIron(III)-porphyrin hydrate with t-BuOOH in aqueous solution. *J. Am. Chem. Soc.* **115**, 21-29.
51. Jones, P. & Suggett, A. (1968). The catalase-hydrogen peroxide system. *Biochem. J.* **110**, 621-629.
52. Saunders, B.C., Holmes-Siadle, A.G. & Stark, B.P. (1964). *Peroxidase*, pp. 134-140, Butterworths, London.
53. Margalit, R., Shaklai, N. & Cohen, S. (1983). Fluorimetric studies on the dimerization equilibrium of protoporphyrinIX and its haematoderivative. *Biochem. J.* **209**, 547-552.
54. Wellinger, R.J. & Sen, D. (1997). The DNA structures at the ends of eukaryotic chromosomes. *Eur. J. Cancer* **33**, 735-749.
55. Li, Y. & Sen, D. (1998). The *modus operandi* of a DNA enzyme. Enhancement of substrate basicity. *Chem. Biol.* **5**, 1-12.
56. Li, Y. (1997). *Catalytic DNA Molecules for Porphyrin Metallation.* Ph.D. Thesis, Simon Fraser University, Burnaby.
57. Corwin, A.H., Chivvis, A.B., Poor, R.W., Whitten, D.G. & Baker, E.W. (1968). The interpretation of porphyrin and metalloporphyrin spectra. *J. Am. Chem. Soc.* **90**, 6577-6583.

58. Saunders, B.C., Holmes-Siadle, A.G. & Stark, B.P. (1964). *Peroxidase*, pp. 112-123, Butterworths, London.
59. Antonini, E. & Brunori, M. (1971). *Hemoglobin and Myoglobin in Their Reactions with Ligands*, North-Holland Publishing Co., Amsterdam.
60. Saunders, B.C., Holmes-Siadle, A.G. & Stark, B.P. (1964). *Peroxidase*, pp. 214-252, Butterworths, London.
61. Rousseau, D.L., Takahashi, S., Wang, J., Ishikawa, K., Yoshida, T., Host, J.R. & Ikeda-Saito, M. (1994). Heme-heme oxygenase complex. *J. Biol. Chem.* **269**, 1010-1014.
62. Adar, F. (1978). Electronic absorption spectra of hemes and hemoproteins. In *The Porphyrins*. (Dolphin, D., ed.), pp. 167-209, Academic Press, New York.
63. Champion, P.M., Marikis, D., Springer, B.A., Egeberg, K.D. & Sligar, S.G. (1990). Resonance raman studies of iron spin and axial coordination in distal pocket mutants of ferric myoglobin. *J. Biol. Chem.* **265**, 12143-12145.
64. Anni, H. & Yonetani, T. (1987). Yeast cytochrome c peroxidase. *J. Biol. Chem.* **262**, 9547-9554.
65. Smith, K.M. (1975). *Porphyrins and metalloporphyrins*, pp. 871-889, Elsevier Scientific Publishing Co., New York.
66. Tamakage, K., Komagoe, K. & Rafiquzzaman, M. (1995). Comparative catalytic activity of hemin and hematin in the breakdown of methyllinoleate hydroperoxide and peroxidation in methanol. *Chem. Pharm. Bull.* **43**, 905-909.
67. Childs, R.E. & Bardsley, W.G. (1975). The steady-state kineticsof peroxidase with ABTS as chromagen. *Biochem. J.* **145**, 93-103.
68. Childs, R.E. & Bardsley, W.G. & Shindler, J.S. (1976). Peroxidase from human cervical mucus. *Eur. J. Biochem.* **65**, 325-331.

Because *Chemistry & Biology* operates a 'Continuous Publication System' for Research Papers, this paper has been published via the internet before being printed. The paper can be accessed from http://biomednet.com/cbiology/cmb – for further information, see the explanation on the contents pages.